REPORT DOCUMENTATION PAGE

Form Approved
OMB No. 0704-0188

1. AGENCY USE ONLY (Leave blank)	2. REPORT DATE	3. REPORT TYPE AND DATES COVERED

4. TITLE AND SUBTITLE

Photorefractive Nonlinear Optics

5. FUNDING NUMBERS

DAAL03-91-G-0243

6. AUTHOR(S)

Mark Cronin-Golomb

7. PERFORMING ORGANIZATION NAME(S) AND ADDRESS(ES)

Electro-Optics Technology Center
Tufts University
4 Colby Street
Medford, MA 02155

8. PERFORMING ORGANIZATION REPORT NUMBER

9. SPONSORING / MONITORING AGENCY NAME(S) AND ADDRESS(ES)

U.S. Army Research Office
P. O. Box 12211
Research Triangle Park, NC 27709-2211

10. SPONSORING / MONITORING AGENCY REPORT NUMBER

ARO 28526.16-PH

11. SUPPLEMENTARY NOTES

The views, opinions and/or findings contained in this report are those of the author(s) and should not be construed as an official Department of the Army position, policy, or decision, unless so designated by other documentation.

12a. DISTRIBUTION / AVAILABILITY STATEMENT

Approved for public release; distribution unlimited.

12b. DISTRIBUTION CODE

13. ABSTRACT *(Maximum 200 words)*

This research program resulted in the development of several new photorefractive devices, and an increase in basic understanding of photorefractive nonlinear interactions. We developed an interferometric phase conjugationg ellipsometer which also led to a new highly accurate class of interferometer applicable to polarimetry and distance measurement. The effectiveness of photorefractive beam cleanup was investigated, and found to be most useful for highly aberrated beams. We investigated the feasibility of efficient self aligning coupling of multiple beams simultaneously into a single single mode fiber. This has applications to fiber optic communications. We studied methods of broadening the spectral bandwidth of volume holographic devices by using achromatic techniques. Applications are in self-pumped phase conjugation of trains of femtosecond pulses, and high data rate transmission in optical fibers. The photorefractive beam propagation method was developed as a tool to analyze photorefractive devices and effects involving large bandwidth signals. It was also applied to model amplified photorefractive scattering (fanning) and the double phase conjugate mirror. A successful statistical model of fanning was developed and tested. We have also begun to study photorefractive waveguides, both epitaxially grown and self induced. High resolution X-ray topography was used to investigate photorefractive crystals and waveguides. A new method for nonvolatile data storage in photorefractive crystals was discovered and theoretically analyzed.

14. SUBJECT TERMS	15. NUMBER OF PAGES
Physics, nonlinear Optics, photorefractive crystals	23
	16. PRICE CODE

17. SECURITY CLASSIFICATION OF REPORT	18. SECURITY CLASSIFICATION OF THIS PAGE	19. SECURITY CLASSIFICATION OF ABSTRACT	20. LIMITATION OF ABSTRACT
UNCLASSIFIED	UNCLASSIFIED	UNCLASSIFIED	UL

NSN 7540-01-280-5500

Standard Form 298 (Rev 2-89)
Prescribed by ANSI Std 239-18
298-102

Photorefractive Nonlinear Optics

Final Report

Mark Cronin-Golomb

March 2, 1995

US Army Research Office

DAAL03-91-G-0243

Electro-Optics Technology Center
4 Colby Street
Tufts University
Medford, MA 02155

LIST OF ILLUSTRATIONS

STATEMENT OF THE PROBLEM STUDIED

The problems studied in this research program were:

a) To investigate nonlinear photorefractive nonlinear optical interactions as they relate to photorefractive devices such as phase conjugate mirrors and image processors.

b) To determine the feasibility of producing practical photorefractive devices and

c) To apply high resolution synchrotron X-ray topography to studies of photorefractive crystals and films.

SUMMARY OF THE MOST IMPORTANT RESULTS

Phase conjugate interferometry and ellipsometry

In the previous contract period, we developed a phase conjugate interferometer for measuring the optical properties of moderately reflecting thin films deposited on transparent substrates. We have continued this research to develop a phase conjugate interferometric ellipsometer suitable for the measurement of films on opaque substrates and for highly transparent films. The device is based on the interferometric ellipsometer of Hazelbroek and Holscher[1]. The end mirror after the sample is replaced by a polarization preserving phase conjugate mirror. (Figure 1) Using a phase conjugate mirror in place of a conventional mirror has many advantages. One is that the sampling arm is self aligning because the phase conjugate beam retraces the path of incidence exactly so that no careful alignment is needed even when changing the sample. This makes possible real time evaluation of films during deposition. Also, most of the distortions caused by substrate irregularities and other imperfections in the optical system including viewports in growth chambers are cancelled by phase conjugation.
A technical point to be considered is that photorefractive phase conjugate mirrors generally work only for one polarization direction. A polarization preserving photorefractive phase conjugate mirror can however be made by using the Basov[2] scheme. Another point is that self pumped phase conjugate mirrors frequently have temporal instabilities both in phase and amplitude of the reflection. Fortunately, phase instability does not affect measurement results because only the phase difference between the two detector outputs is used. Meanwhile, drift in the reflectivity can be controlled to within 0.1% during a period of one minute which is plenty of time for completion of a measurement by the ellipsometer.

Interferometric Polarimeter

In the course of investigating the interferometric ellipsometer, we invented a new type polarimeter for measuring the polarization state of quasimonochromatic light. This phase shifting elliptic

interferometer (PEI) can measure the polarization state of light quickly with high accuracy. We expect that it will be fast, compact and relatively inexpensive.
The conventional technique for measuring polarization state is to align a rotatable waveplate and linear polarizer followed by a photodetector in the optical path of the beam. Measurements are made of waveplate and polarizer angle at nulls of the intensity at the photodetector. This technique, although well developed in automated instruments, is time consuming and somewhat expensive.

Figure 2 shows the layout of the PEI which is basically a Michelson interferometer in which both polarization components travel common paths. The waveplate in one arm switches the s and p polarizations in that arm so that the interferences in the interferometer outputs give the relative amplitudes of both input components as well as the phase difference between them. The two detectors measure the same quantities but in different quadratures at the same time. The detector combination thus never needs biasing to obtain maximum sensitivity.

The device several positive features:

i) The measurement is independent of vibration in the system and linearity of the piezoelectric phase shifting element. This is accomplished by plotting the outputs of the detectors against each other, forming an ellipse. The polarization state can be found by fitting ellipse parameters. This robustness comes about because the interferometer is common path for the s and p components and the detector outputs are measured simultaneously. To show this, we made an experimental demonstration on an optical table without vibration isolation.

ii) The effects of angular misalignments of the input beam cancel each other out if the path lengths in both arms are equalized. A compact version of the device would be very easy to use, just like a photodetector.

iii) The polarization ellipse can be displayed on a monitor during data acquisition. This is useful for checking the reliability of the device.

Double quadrature interferometry

The common path and dual quadrature characteristics of the polarimeter described above can be useful for many other types of interferometers such as position sensors. We expect that such devices will have 0.1nm sensitivity, 1nm accuracy, and range equal to half the coherence length of the laser used.

Beam propagation method for photorefractive nonlinear optics

In order to gain a better understanding of broadband effects in photorefractive devices, we developed a beam propagation method for optical interactions in photorefractive crystals. This enabled us to include the effects of diffractive propagation in these devices. These effects can be expected to become important for beams with very fine scale structure such as speckle beams and beams carrying very finely spaced image details such as those that might be used in photolithography. The basic idea is to use a split step method in which the nonlinearities are modelled as being concentrated into thin transparencies equally spaced along the propagation direction. In between the nonlinear transparencies, the medium is modelled as being uniform so

that a translation invariant propagation kernel can be used. In this case, diffractive propagation can be calculated by using fast Fourier transform methods. We first used the method to investigate our experimental results on short pulse[3] and low coherence beam coupling[4].
With the tool in hand, we then applied it to investigations of image fidelity in two beam coupling image amplification and phase conjugation as well as to models of photorefractive amplified scattering (fanning).

Applications of the beam propagation method

Four-wave mixing and the double phase conjugate mirror.

We extended the two-beam coupling beam propagation method to four-wave mixing by using a relaxation method to handle the associated two-point boundary value problem. Our new model matches the predictions of the plane wave theory well in the cases where the two models apply. We then developed a model of the amplified scattering (fanning)[5]. This model is necessary to describe the seeding of self-pumped phase conjugators. The scatterers are described as a set of phase screens, at the surface of the crystal to simulate surface scattering, and distributed throughout the volume of the crystal to simulate volume scattering. The phase screens are designed to give the same amplitude and correlation lengths as observed experimentally, both with and without photorefractive amplification. At present, our model is a scalar model, and so is applicable to cases in which the nonlinearity is essentially scalar, such as in strontium barium niobate where r_{33} is dominant. There were significant differences between the scalar predictions and the observations of fanning in barium titanate, where an essentially vector electrooptic coefficient r_{42} is dominant. A typical calculated image of fanning gratings in a crystal is shown in Fig.3

With this fanning model in hand, we were able to calculate the spatial behavior of the double phase conjugate mirror (DPCM). We have been able to calculate spatial images of the interaction region in the DPCM and connect a time series of these images into an animation. Representative frames of double phase conjugation of two gaussian beams and of double phase conjugation of a gaussian beam and a gaussian beam modulated by a square wave pattern are shown in Fig. 4.

Various one- and two-dimensional analyses of the double phase conjugate mirror (DPCM) have classified it as either an amplifier or an oscillator. We have attempted to bridge the gap in this controversy by two-dimensional scalar numerical simulations of the device for two different cases which have previously been considered to exhibit either amplifier or oscillator behavior: the overlap region of interacting beams lies entirely inside the crystal (amplifier), and the overlap region partially overlaps the input boundaries (oscillator). By defining an oscillator as a device whose output remains high if it is above threshold when its input seeding is cut off, we demonstrate the behavior of the DPCM for both types of interaction regions. Up until the end of 1994, we had been using Connection Machines for these calculations. Now, however, we are running code just as quickly using Fortran-90 on Tufts University's DEC Alpha farm. We are

preparing an abstract and summary for submittal to the 1995 Photorefractive Materials, Effects and Devices Meeting in Estes Park, CO.

The fanning beams usually split up into narrow filaments. In order to investigate the origin of this effect, we generalized the photorefractive model for the beam propagation method to include the effects of secondary trap levels in the photorefractive band conduction model[6]. This model was first introduced to explain the sublinear intensity dependence of the photorefractive effect observed in some experimental set-ups. We performed numerical simulations of beam propagation in photorefractive crystals using this model for the space charge field solution. Find that the intensity distribution of beam fanning is shifted to higher angles compared to the intensity distributions of fanning obtained using the single trap model. These results will be presented at the 1995 CLEO meeting in Baltimore in a paper entitled "Photorefractive beam propagation using secondary trap model".

Accurate algorithms for calculating the repetitive Fourier Transforms in the beam propagation method are required. As part of an effort to improve our calculational accuracy, we have completed research on numerical evaluation of the zero-order Hankel transform using Filon quadrature philosophy in collaboration with Richard Barakat. A manuscript is to be submitted to the Journal of Computational Physics describing the derivation of a numerical algorithm that is based on the Filon method for evaluating oscillatory integrals. Its results show greatly improved numerical accuracy compared to previously used methods.

Femtosecond temporal encoding in photorefractive crystals.

As part of our attempt to mode lock a semiconductor ring laser with an intracavity distortion correcting DPCM, we carried out an experimental investigation of the feasibility of writing volume holograms with ultrshort pulses[7]. We found that in femtosecond pulse trains could indeed write holograms in photorefractive crystals in spite of the fact that the 5mm crystals were about 300 times longer than the 50fs pulses used in the experiment. Femtosecond pulses diffracting from these holograms would diffract into pulses only slightly longer than the original writing pulses, with diffraction efficiencies very close to those obtainable with continuous wave illumination. Temporal sequences of femtosecond pulses could also be reconstructed. The reason is that the shortness of the pulses does not shorten the interaction length, although it does restrict the dimension of the grating perpendicular to the interaction length. It is the interaction length, not the perpendicular dimension of the grating that principally determines the diffraction efficiency.
One application of pulse sequence storage is to record fine scale range information, as would be useful in imaging of sructures in scattering media, such as ocular retinas. This is also closely related to the recently investigated coherence microscopy that is under current investigation for biomedical applications.

Two beam coupling with beams of reduced spatial coherence

In the previous contract, we started investigations of the effects of low spatial coherence on two beam coupling. This question is of importance in considering whether our achromatic holography technique would work with white light in the spatially incoherent sense. It is also relevant to the effectiveness of photorefractive devices for multimode fibers in which modal scrambling is important. In this contract period, we extended our results to a two dimensional theory, first in a quasiplane wave undepleted pump approximation and then to the full theory with pump depletion and diffractive propagation using the beam propagation method[8]. We found that the nonlinear interaction increased the spatial coherence of the amplified beam, and reduced the spatial coherence of the deamplified beam. This is because the amplification process favors the stronger of monochromatic components of the signal, so that the signal becomes more spatially coherent. However there is also some loss of image information.

Achromatic double phase conjugate mirror

Following on our work of the previous contract, we have extended our research on achromatic volume holography to the case of the double phase conjugate mirror[9]. It is possible to make the DPCM achromatic using material dispersion without the use of an auxiliary fixed grating. This advance improves the prospects of making high fidelity self pumped phase conjugate mirrors pumped by broadband light sources such as femtosecond pulse trains and rapidly modulated optical carriers for optical communication.

Efficient self aligning coupling to single mode fibers

In collaboration with Baruch Fischer at the Technion, Israel, we have investigated the suitability of the double phase conjugation for multi-beam coupling into a single mode fiber[10]. The ability to couple many data channels into a single single mode fiber can be useful, for example in the case of vertical cavity laser arrays (VCSEL) so that the entire matrix of beams emitted by the VCSEL can be coupled at the same time into the fiber. Each of the channels may be independently modulated so that the fiber will carry the data of all channels which may be demultiplexed further down the transmission line. We found that the Fresnel corrected insertion efficiency was over 97%. The transmission efficiency of the double phase conjugate mirror (DPCM) was 40% (Fresnel corrected) so that the overall efficiency was 39%. The fact that phase conjugation is used means that the system is sell aligning, and tolerant of small changes. One possible concern about a limitation of this technique is one of bandwidth. Normally, a volume hologram has a relative bandwidth equal to the inverse of the number of wavelengths along the interaction length. In the typical case of a 5mm long crystal, this amounts to a relative bandwidth of about $2x10^{-4}$, or 60Ghz for $1\mu m$ radiation. This is a relatively small bandwidth for a fiber optic system. However, by using an achromatic DPCM, the bandwidth can be extended to many terahertz.

Photorefractive surface waves

Solitary waves in photorefractive media have recently been the subject of several theoretical and experimental investigations [11]. Their appearance requires that the nonlinear response is predominantly in phase with the optical excitation so that the diffusion component of the space charge field is negligible compared to the drift component. A Gaussian beam launched

into a photorefractive crystal with diffusion nonlinearity will be deflected in the direction of positive gain and depending on the strength of the nonlinearity, the beam will either be focussed or defocussed. At a critical nonlinearity, the beam will maintain its width as it travels[12]. If such a beam meets the crystal surface so that it is totally internally reflected, one might expect that the beam would be guided along the surface in the same way that a Kerr medium can guide light along a nonlinear interface[13] . We have found theoretically the existence of such photorefractively induced waveguides and describe their properties.

In the first approach, photorefractive beam propagation method is used to test for their existence. Figure 5 shows the development of a guided wave along an interface in which the refractive index of the photorefractive medium is 2.36 and the input beam is gaussian of waist 2μm, positioned initially 2μm away from a refractive index discontinuity of 0.1. The method uses Fast Fourier Transform beam propagation and a fully nonlinear rate equation model of the photorefractive nonlinearity. The results are compatible with the existence of guided waves.
The second approach is based on the fact that the photorefractive paraxial wave equation remains linear and homogeneous if a logarithmic model of the nonlinearity is used [14]:

$$E_{sc}(x) \propto \frac{1}{I}\frac{dI}{dx}$$

where E_{sc} is the space charge field and I is the local intensity. This approximation requires that the intensity overcomes the dark conductivity and that the field does not change rapidly on the scale of the Debye length. Here, as in reference 14 where bistability at a photorefractive interface was considered, the model assumes that the photorefractive charge carriers can diffuse across the crystal interface so that the boundary conditions are compatible with the logarithmic model. The eigenmodes of photorefractively induced waveguide decay exponentially away from the boundary. The decay distance d can be interpreted as the width of the photorefractively induced waveguide.

$$d=\left[\left(\frac{2\pi n}{\lambda}\right)^2 r\frac{k_B T}{e}\right]^{-1}$$

where λ is the wavelength, n is the crystal refractive index, k_B is Boltzmann's constant T is the temperature, and r is the electrooptic coefficient. For parameters typical of barium titanate in the visible, d is approximately 5μm.
In the TE case the dispersion relation for the guided modes is

$$\beta_x=\sqrt{\left(\frac{2\pi n}{\lambda}\right)^2-\frac{1}{d^2}-\beta_z^2}$$

where β_x is the transverse mode wavenumber and β_z is the longitudinal mode wavenumber.

This method of waveguide induction may lead many other phenomena, such as photorefractive interactions between guided beams including two beam coupling and phase conjugation with the increased speed associated with optical confinement. Also, photorefractive solitary waves may be able to be induced in the guide, perhaps by the quadratic photorefractive

effect.

Photorefractive two beam coupling beam cleanup

One known method for laser beam cleanup is via two beam coupling with photorefractive crystals. In the process, energy transfer occurs between a strong pump beam and a weak signal beam without phase cross-talk so that a clean signal beam can be amplified by a phase aberrated pump beam without degradation of its beam quality. One of the concerns about this method is whether it is effective compared to other laser beam cleanup methods and under what circumstances it works well. Several experimental and theoretical studies have been done in this area[15 16] and image amplification[17 18 19].. Previously, fidelity of the amplified beam to the weak signal beam has only been measured qualitatively by interferometric means and for specific beam input ratios[15 16]. To accurately estimate the efficiency of the method, the amplified beam quality has to be measured quantitatively and the influence of beam input ratio on overall efficiency must be considered.

We have performed an experimental evaluation of effectiveness of photorefractive two beam coupling laser beam cleanup. In order to estimate the effectiveness quantitatively, we use M^2 , the times-diffraction-limit number, as a measure of the quality of the laser beam and introduce a Figure of Merit (FOM) of the beam defined as Intensity/$(M^2)^2$. We also compared the efficiency of this method to that of spatial filtering as a typical method of laser beam cleanup.

We found no significant difference in beam cleanup efficiency between two beam coupling and spatial filtering for weakly aberrated beams whose M^2 ranges from 2 to 5, even when fanning was eliminated as a noise source by using tightly focussed beams (Fig 6). This may be due to the fact that one needs substantial overlap between the aberrated pumps and the clean signal, something which is difficult to achieve sufficiently effectively with mildly aberrated pump beams. We are in the process of evaluating this effect with the beam propagation model. When we considered the case of a severely aberrated beam, two beam coupling could do much better than a spatial filter. For a beam that was aberrated to 700 times diffraction limit by passage through Scotch Tape, the improvement in figure of merit was by a factor of about 10. The overall power transfer form the aberrated beam to the clean signal was 3.8%.

Birefringent phase matching for nonvolatile readout of holographic memories

One attractive application of photorefractive materials is for use in optical memory storage. Holographic storage in photorefractive materials offers high storage density and fast readout rate, due to the three dimensional storage and parallel retrieval, possible in photorefractives. Photorefractive materials, such as lithium niobate, can potentially store data for long periods of time, as methods for fixing the photorefractive gratings are developed. When the fixing problem is overcome, photorefractive memory storage may offer a significant improvement over standard data storage techniques. Thus, researchers are looking carefully at techniques for memory storage and retrieval in volume holograms.

To prolong the lifetime of stored holograms, it would be advantageous to read them out at a wavelength that would not erase the grating. Efficient storage, on the other hand requires that the

holograms be written at a wavelength where the crystal is photorefractively sensitive. This means that it would be preferable to write the data in with, say green light, and read it out with say, red light. Phase matching angles for red readout beams can easily be found for holograms of a plane waves written with green light. But the image, or data field will actually be more complicated than a single plane wave. Only one of the plane wave components of a complicated image can usually be phase matched by a plane wave red readout beam. This problem has been addressed by several researchers, who have used spherical readout beams, and multihologram recording per page[20].

We have a different approach to the problem, whereby we use crystal birefringence to allow image phase matching at both the recording and readout wavelengths. By recording the hologram with ordinary polarized light and reading it with extraordinary polarized light, we can extend the image readout phase matching angles. Figure 7a shows the usual situation, while Fig. 7b shows the extended phase matching case. The circles and ellipses in Fig. 7b are the index ellipsoid cross sections for ordinary and extraordinary polarization. For this scheme to work, there must be points where the curvature of the extraordinary ellipse is the same as the curvature of the ordinary circle. It can be shown that such points exist for extraordinary and ordinary beams with wavelengths satisfying

$$\frac{n_o(\lambda_{ext})}{n_o(\lambda_{ord})n_e(\lambda_{ext})} < \frac{\lambda_{ext}}{\lambda_{ext}} < \frac{n_o(\lambda_{ord})}{n_o(\lambda_{ord})n_o(\lambda_{ext})}$$

Figure 8 shows the wavelength ranges over which such phase matching is possible. For example, it is possible to write with extraordinary yellow light at 590nm and readout with ordinary red light at 633nm. An experimental investigation of this effect is currently under way.

X-Ray topography of photorefractive crystals

We have continued our collaboration with NIST on the use of high-resolution x-ray diffraction imaging to examine crystallographic features in photorefractive crystals. We have imaged lattice imperfections in the photorefractive materials barium titanate and strontium barium niobate. Anti-parallel ferroelectric domains were observed in the bulk for the first time, and their visibility explained in terms of the coupled-mode theory of dynamical x-ray diffraction. The technique was also used to image directly the photorefractive space-charge field, and the results were explained in terms of the coupled-mode theory and a new solution of the strain problem in photorefractive crystals. It turns out that surface strain effects are very important in the interpretation of reflection images. The lattice deformations are significantly higher than one would expect from a bulk crystal model. The magnitude of the space-charge field was determined, and compared with the results of numerical solutions of the standard charge transport model of photorefractive grating formation.

Thin film electrooptic materials and waveguides

We have started a collaboration with a Boston area company, NZ Applied Technologies in an effort to grow and characterize thin film electro-optic materials. Applications of these materials include efficient compact electrooptic modulators and integrated optic photorefractive

devices such as phase conjugate mirrors. We have used synchrotron X-ray topography to investigate the quality of epitaxial $Sr_xBa_{1-x}Nb_2O_6$ (SBN) films grown by plasma enhanced MOCVD[21]. Figure 7 shows topograph of (002) and (004) lattice planes of a 1.5μm SBN (x=0.60) film and the MgO substrate respectively. The large grainlike features are due entirely to irregularities in the substrate. The epitaxy of the film is seen to be excellent.

REFERENCES

1. H.F. Hazebroek and A.A. Holscher, J. Phys. E. **6**, 822 (1973)

2. N.G. Basov, V.F. Efimkov, I.G. Zubarev, A.V. Kotov, S.I. Mikhailov, and M.G. Smirnov, JETP Lett **28**, 197 (1978)

3. L.H. Acioli, M. Ulman, E.P. Ippen, J.G. Fujimoto, H. Kong, B.S. Chen, and M. Cronin-Golomb, Opt. Lett. 16, 1984 (1991)

4. M. Cronin-Golomb, H. Kong, and W. Krolikowski, J. Opt. Soc. B 9, 1698 (1992)

5. E. Parshall, M. Cronin-Golomb, and R. Barakat, to be published, Opt. Lett.

6. Brost, G.A.; Motes, R.A.; Rotge, J.R., JOSA **B9**, 1879 (1988)

7. L.H. Acioli, M. Ulman, E.P. Ippen, J.G. Fujimoto, H. Kong, B.S. Chen, and M. Cronin-Golomb, Opt. Lett. 16, 1984 (1991)

8. M. Cronin-Golomb, H. Kong, and W. Krolikowski, J. Opt. Soc. B 9, 1698 (1992)

9. H. Kong, M. Cronin-Golomb and B. Fischer, Opt. Commun. 93, 92 (1992)

10. M. Snowbell, N. Strasman, B. Fischer, and M. Cronin-Golomb, Journ. Lightwave Tech. 13, 55 (1995)

11. B. Crosignani, M. Segev, D. Engin, P. DiPorto, A. Yariv, and G. Salamo, J. Opt. Soc. Am. **B10**, 446 (1993)

12. D.N. Christodoulides and M.I. Carvalho, Opt Lett. **19**, 1715 (1994)

13. G.I. Stegeman, C.T. Seaton, J. Arisayu, R.F. Wallis, and A.A. Maradudin, J. Appl. Phys. **58**, 2453 (1985)

14. R. Daisy and B. Fischer, J. Opt. Soc. Am. **B11**, 1059 (1994)

15. A.E.T. Chiou and P. Yeh, Opt. Lett. **10**, 621 (1985)

16. A.E. Chiou and P. Yeh, Opt. Lett. **11**, 461 (1986)

17. F. Vacchs and P. Yeh, J. Opt. Soc. Am. **B6**, 1834 (1989)

18. G. Notni and R. Kowarschik, IEEE J. Quantum Electron. **QE27**, 2193 (1991)

19. S. Zhou, Q.B. He and P. Yeh, Opt. Commun. 99, **18** (1993)

20. D.Psaltis, D., F. Mok, and H.-Y.S Li, Opt. Lett.**19**, 210 (1994)

21. L.D. Zhu, J. Zhao, S.B. Kang, Wang, M. Sinclair, D. Dimos, G.D. Fogarty, M. Cronin-Golomb, B. Steiner, P.E. Norris, B. Kear, and B. Gallois. submitted to Applied Physics Letters

LIST OF ALL PUBLICATIONS AND TECHNICAL REPORTS

Submitted

"Epitaxial electro-optical $Sr_xBa_{1-x}Nb_2O_6$ films by single source plasma enhanced metalorganic chemical vapor deposition" L.D. Zhu, J. Zhao, S.B. Kang, Wang, M. Sinclair, D. Dimos, G.D. Fogarty, M. Cronin-Golomb, B. Steiner, P.E. Norris, B. Kear, and B. Gallois. submitted to Applied Physics Letters

In Press

"A model of amplified scattering in photorefractive media: comparison of theory and experiment", E. Parshall, M. Cronin-Golomb, and R. Barakat, Optics Letters

Published

"Phase conjugate interferometric analysis of thin films", E. Parshall and M. Cronin-Golomb, Appl. Opt. 30, 5090 (1991)

"Photorefractive two beam coupling with reduced spatiotemporal coherence" H. Kong, C. Wu, and M. Cronin-Golomb, Opt. Lett. 16, 1183 (1991)

"Femtosecond temporal encoding in barium titanate", L.H. Acioli, M. Ulman, E.P. Ippen, J.G. Fujimoto, H. Kong, B.S. Chen, and M. Cronin-Golomb, Opt. Lett. 16, 1984 (1991)

"Experimental study of achromatic volume holography with dispersive compensation in barium titanate", H. Kong, C. Wu, and M. Cronin-Golomb, Opt. Lett. 17, 297 (1992)

"Photorefractive wave mixing with finite beams" W. Krolikowski, M. Cronin-Golomb, Opt. Commun. 89, 88 (1992)

"Whole beam method for photorefractive nonlinear optics", M. Cronin-Golomb, Opt. Commun. 89, 276 (1992)

"Achromatic double phase conjugate mirror", H. Kong, M. Cronin-Golomb and B. Fischer, Opt. Commun. 93, 92 (1992)

"Photorefractive two-beam coupling with light of partial spatiotemporal coherence", M. Cronin-Golomb, H. Kong, and W. Krolikowski, J. Opt. Soc. B 9, 1698 (1992)

"Analysis of metal clad antiresonant reflecting optical waveguide for polarizer applications", U. Trutschel, M. Cronin-Golomb, G. Fogarty, F. Lederer, M. Abraham, Phot. Tech. Lett. 5, 336 (1993)

"Observation of chaos in off bragg photorefractive four-wave mixing, K.D. Shaw, Opt. Commun, 97 148 (1993)

"Soliton-like optical switching in circular nonlinear fiber array", W. Krolikowski, U. Trutschel, M. Cronin-Golomb, and C. Schmidt-Hattenberger, Opt. Lett. 19, 320 (1994)

"Efficient self-aligning multi-mode beam coupling into a single mode fiber", M. Snowbell, N. Strasman, B. Fischer, and M. Cronin-Golomb, Journ. Lightwave Tech. 13, 55 (1995)

Book Chapters

"Self-Pumped Phase Conjugate Mirrors and Other Oscillators", M. Cronin-Golomb, to appear in "Phase Conjugation", ed D. Proch and M. Gower (Springer Verlag 1994)

"Photorefractive Materials and Devices", M. Klein and M. Cronin-Golomb, "Handbook of Optics", ed M. Bass (McGraw Hill, 1994)

Theses

"Temporal and spatial coherence effects in photorefractive nonlinear optics", Hongzhi Kong, Ph.D Thesis (1991)

"High-Resolution X-Ray Diffraction Imaging of Photorefractive Crystals and Gratings" Gerard D. Fogarty, Ph.D Thesis (1994)

LIST OF ALL PARTICIPATING SCIENTIFIC PERSONNEL SHOWING ANY ADVANCED DEGREES EARNED BY THEM WHILE EMPLOYED ON THE PROJECT

M. Cronin-Golomb (Principal Investigator)

Visiting Scientists:
Qiushui Chen
Atsushi Takada
Wieslaw Krolikowski

Graduate Students:
Hongzhi Kong PhD
Elaine.R. Parshall (AASERT)
G. Fogarty (AASERT) PhD
Daniel. Ball
Mark. Tarr

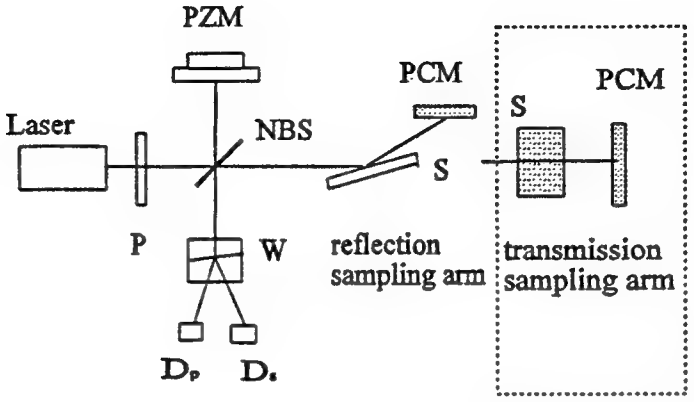

Figure 1. Basic scheme for the interferometric ellipsometer with a phase conjugate mirror in the sampling arm; P, polarizer, NBS, nonpolarizing beamsplitter, W, Wollaston prism, PZM, piezomirror, Dp, Ds, photodetectors, S, sample being tested.

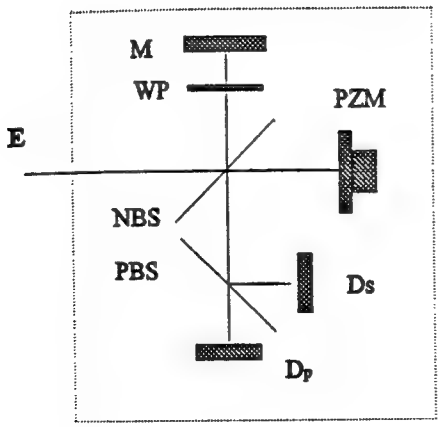

Figure 2. Phase shifting elliptic interferometer (PEI). NBS, nonpolarizing beamsplitter, WP, waveplate, M, reflecting mirror, PZM, piezomirror, PBS, polarizing beamsplitter, Dp, Ds photodetectors.

Figure 3. Calculated fanning beams for 40μm waist laser beam. The amplitude coupling constant γl is 11. The interaction length is 1mm.

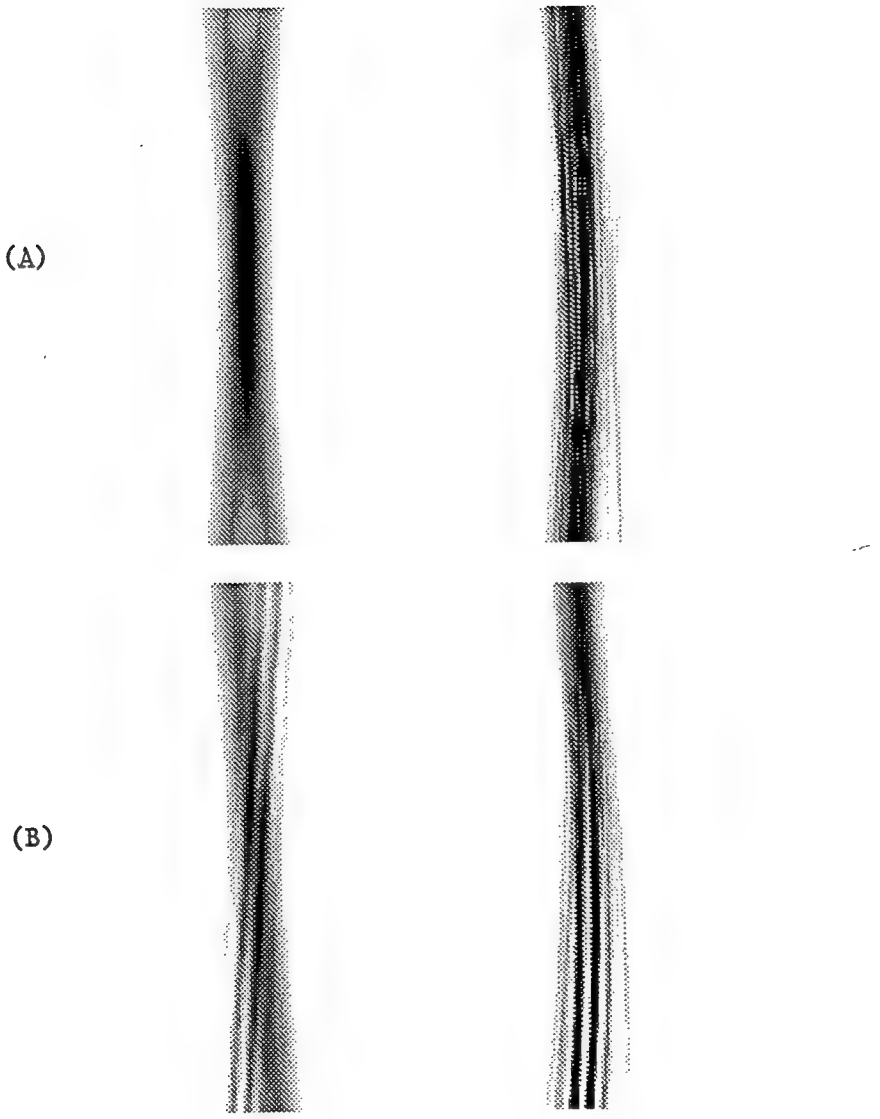

Figure 4. a) Double phase conjugation of two gaussian beams incident from the top and bottom of the figure. γl=15, beam waists 50μm.. The left hand image shows the beams at time 0, the right hand image shows the beams after 6.7 photorefractive time constants.
b) Same as a) except lower gaussian is modulated by a square wave grating. The final state is at 10 photorefractive time constants.

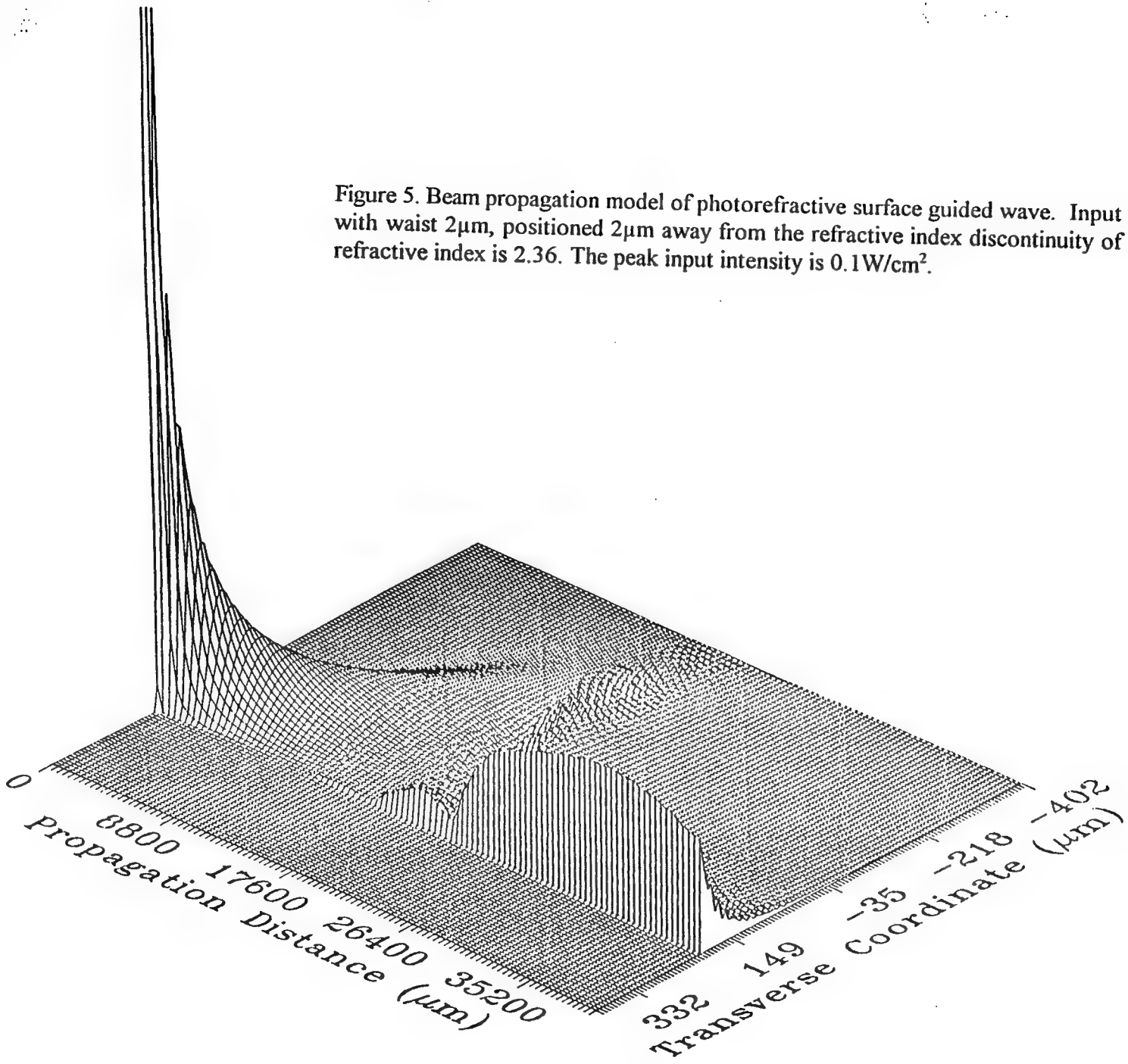

Figure 5. Beam propagation model of photorefractive surface guided wave. Input beam is gaussian with waist 2μm, positioned 2μm away from the refractive index discontinuity of 0.1. The crystal refractive index is 2.36. The peak input intensity is 0.1W/cm^2.

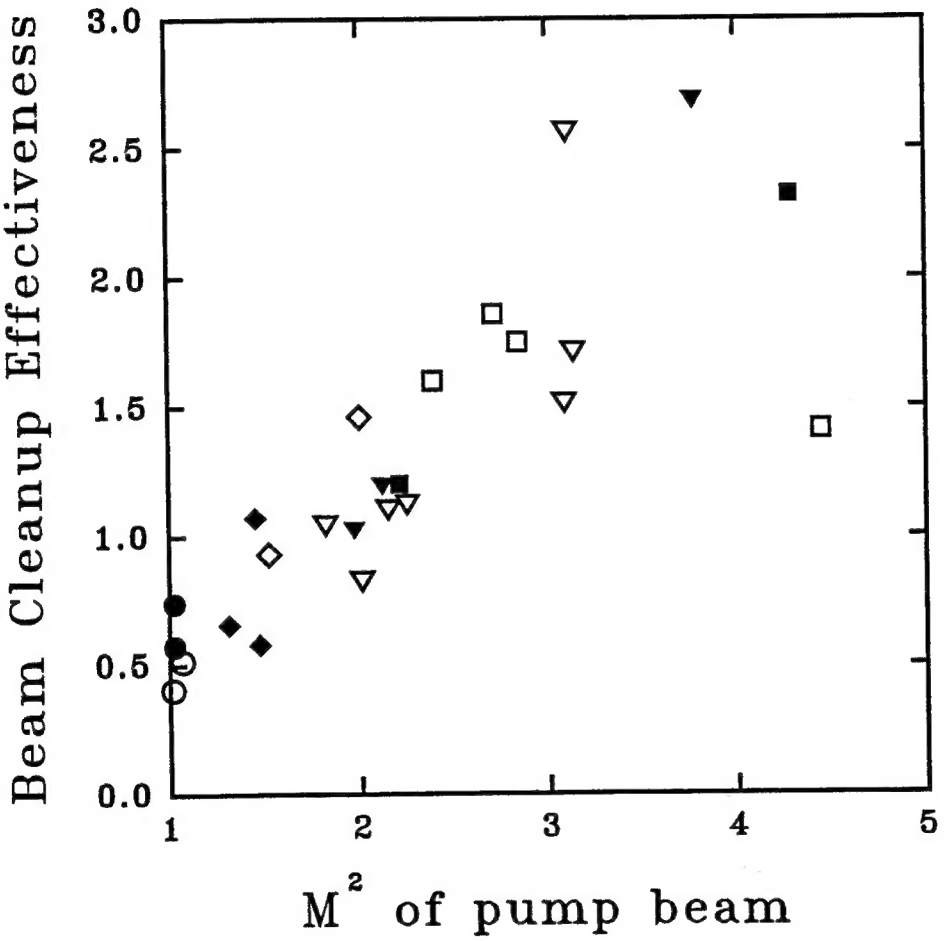

Figure 6. Beam cleanup effectiveness comparison of two beam coupling and spatial filtering. The open points are for two beam coupling and the closed points are for spatial filtering.

(a)

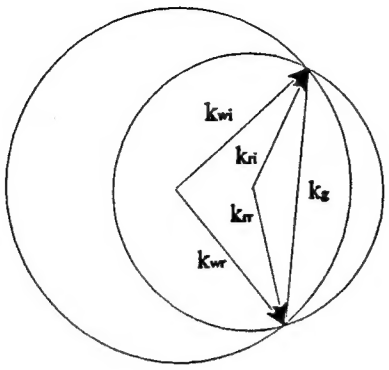

(b)

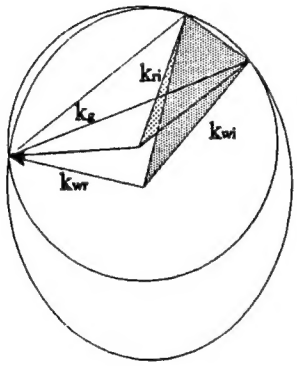

Figure 7 a) Normal phase matching diagram for writing and reading holograms at different wavelengths k_{wi}, image writing wavevector, k_{wr}, reference writing wavevector, k_{rr}, reference reading wavevector, k_{ri}, image reconstructed wavevector, k_g, grating wavevector. The circles are the index ellipsoid cross sections for ordinary polarization. Notice that only one image angle is phase matchable.

b) New phase matching diagram for writing and reading holograms at different wavelengths k_{wr}, reference writing wavevector, k_{rr}, reference reading wavevector,k_{wi}, image writing wavevector range, k_{ri}, image reconstructed wavevector range, kg, grating wavevectors.

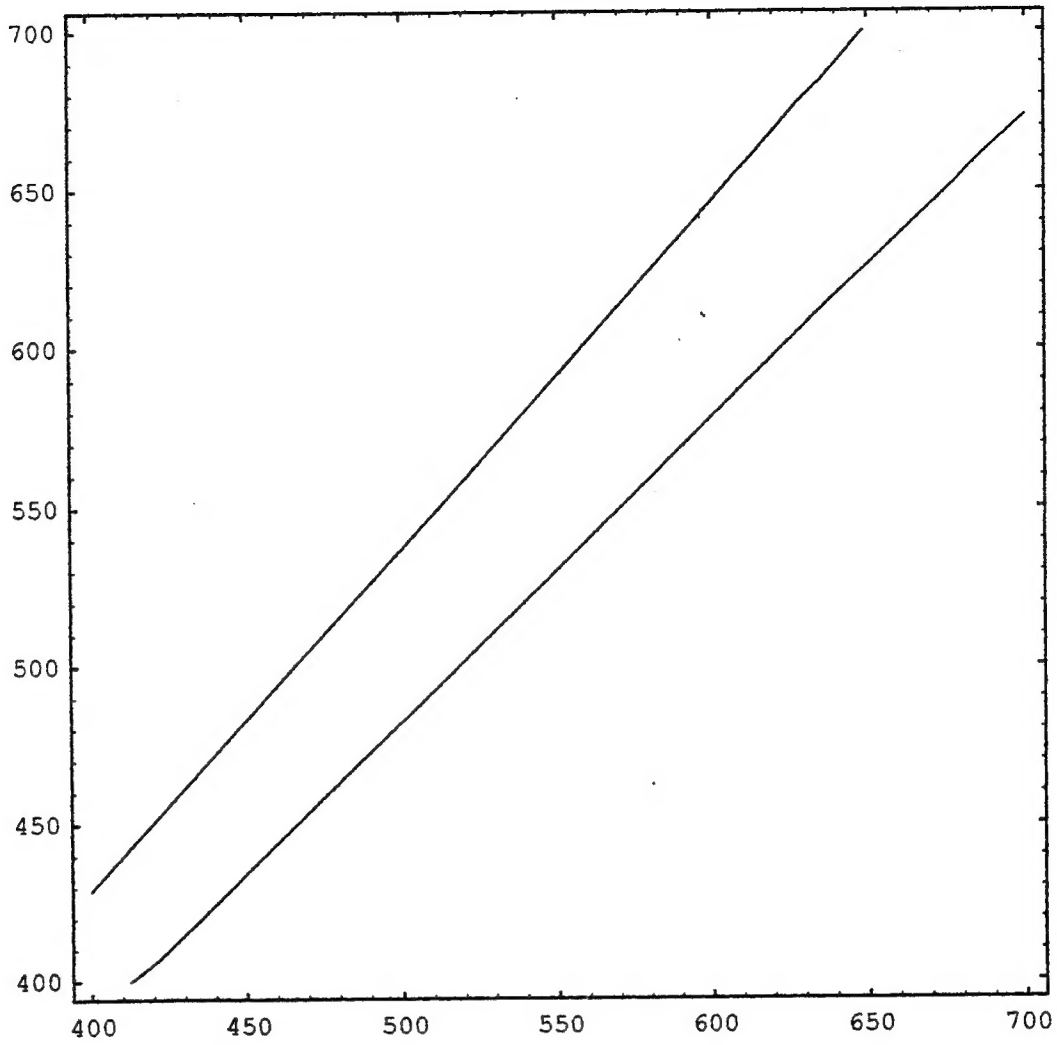

Figure 8 Plot showing range of birefringent phase matching. The wavelength of the extraordinary polarized pair of beams is shown on the horizontal axis, while the wavelength of the ordinary pair is shown on the vertical axis. Wavelength pairs between the two diagonal lines are phase matchable. For example, an extraordinary writing pair at 590nm is phase matchable for ordinary readout at 633nm

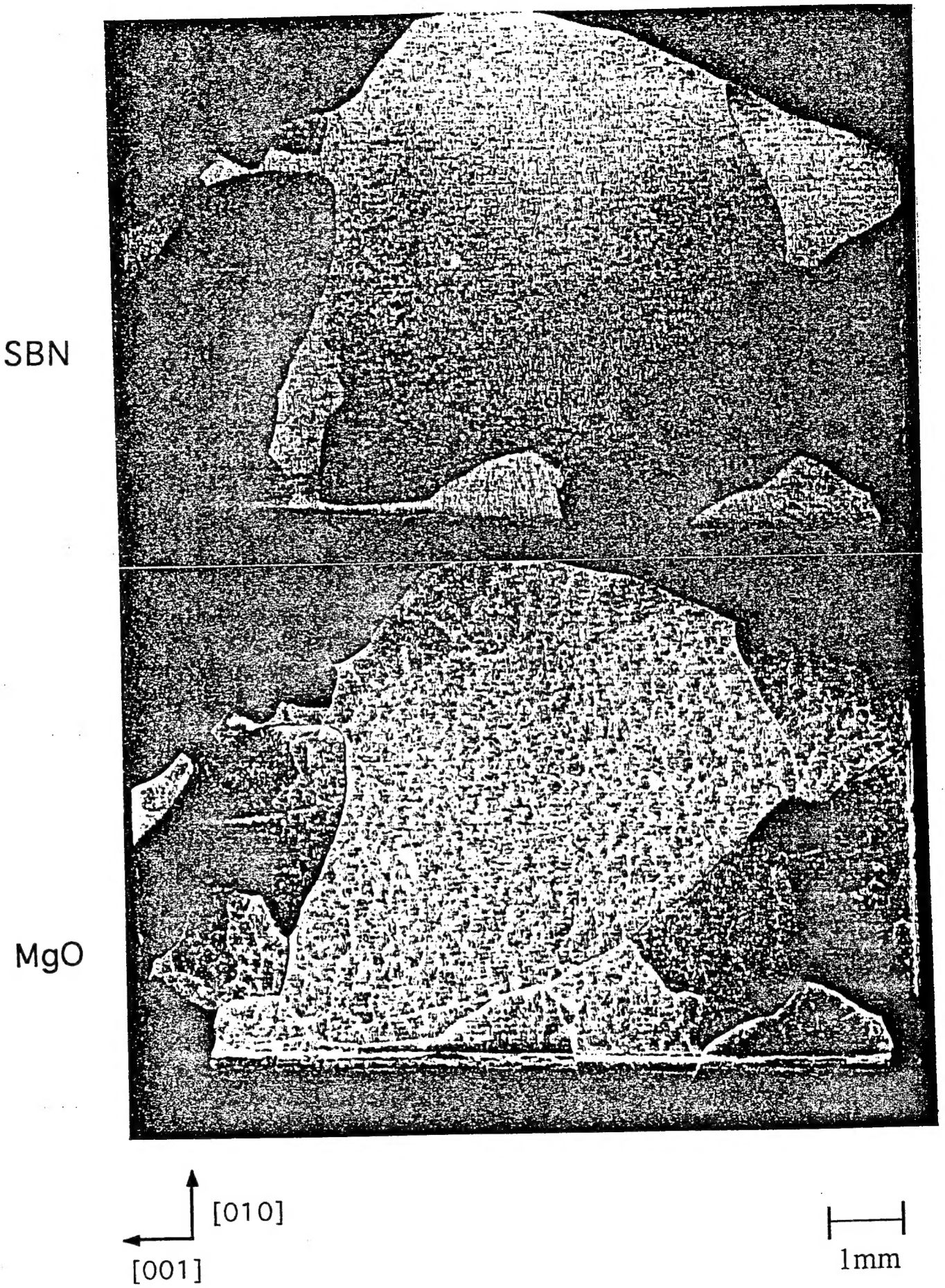

Figure 9. High resolution synchrotron X-ray diffraction image: a) (002) surface of the strontium barium niobate film and b) (004) surface of the MgO substrate.